The human P^k histo-blood group antigen provides protection against HIV-1 infection

Nicole Lund,[1,2] Martin L. Olsson,[3] Stephanie Ramkumar,[1] Darinka Sakac,[2] Vered Yahalom,[4] Cyril Levene,[4] Åsa Hellberg,[3] Xue-Zhong Ma,[5,6] Beth Binnington,[7] Daniel Jung,[8,9] Clifford A. Lingwood,[1,7,10] and Donald R. Branch,[1,2,5,6]

[1]Department of Laboratory Medicine and Pathobiology, University of Toronto, Toronto, ON; [2]Canadian Blood Services, Toronto, ON; [3]Division of Hematology and Transfusion Medicine, Department of Laboratory Medicine, Lund University & University Hospital Blood Centre, Lund, Sweden; [4]Magen David Adom National Blood Services, Ramat Gan, Israel; [5]Department of Medicine, University of Toronto, Toronto, ON; [6]Division of Cell and Molecular Biology, Toronto General Research Institute of the University Health Network, Toronto, ON; [7]Research Institute, Hospital for Sick Children, Toronto, ON; [8]Héma-Québec Research & Development, Québec, QC; [9]Department of Microbiology and Biochemistry, Laval University, Québec, QC; and [10]Department of Biochemistry, University of Toronto, Toronto, ON

Several human histo-blood groups are glycosphingolipids, including P/P1/P^k. Glycosphingolipids are implicated in HIV-host-cell-fusion and some bind to HIV-gp120 in vitro. Based on our previous studies on Fabry disease, where P^k accumulates and reduces infection, and a soluble P^k analog that inhibits infection, we investigated cell surface–expressed P^k in HIV infection. HIV-1 infection of peripheral blood–derived mononuclear cells (PBMCs) from otherwise healthy persons, with blood group P_1^k, where P^k is overexpressed, or blood group p, that completely lacks P^k, were compared with draw date–matched controls. Fluorescence-activated cell sorter analysis and/or thin layer chromatography were used to verify P^k levels. P_1^k PBMCs were highly resistant to R5 and X4 HIV-1 infection. In contrast, p PBMCs showed 10- to 1000-fold increased susceptibility to HIV-1 infection. Surface and total cell expression of P^k, but not CD4 or chemokine coreceptor expression, correlated with infection. P^k liposome–fused cells and $CD4^+$ HeLa cells manipulated to express high or low P^k levels confirmed a protective effect of P^k. We conclude that P^k expression strongly influences susceptibility to HIV-1 infection, which implicates P^k as a new endogenous cell-surface factor that may provide protection against HIV-1 infection. (Blood. 2009;113:4980-4991)

Introduction

HIV-1 infection and development of AIDS vary greatly among persons and populations and are probably, at least in part, dependent on genetic factors.[1] Indeed, the first natural resistance factor reported for HIV infection was a polymorphism within the CCR5 HIV-1 coreceptor gene, termed *CCR5-Δ32*.[1,2]

However, no genetic factors thus far have been able to adequately explain the variability in both in vitro and in vivo susceptibility to HIV-1 infection.[2,3]

There is a longstanding association between pathogens and histo-blood groups, both in protection conferred by a specific blood type and in pathogen interactions with blood group antigens.[4] The P/P1/P^k blood group antigens are of particular interest, with many defined pathogen interactions,[4-7] and an expression profile not limited to erythrocytes. Galabiose (Galα1-4Gal) is the terminal structure of P1 and P^k, also known as globotriaosylceramide (Gb_3) and a marker for germinal center B lymphocytes (CD77).[8] P^k is the precursor for the P antigen, also known as globotetraosylceramide (globoside, Gb_4), which terminates with β1-3GalNAc.[9] P_1 and P_2 are the 2 common P/P1/P^k-related blood group phenotypes. P_1 persons (~ 80% of whites but only ~ 20% of Asians)[6,10] express P and P1 but normally express moderate to low amounts of P^k on their cell surfaces. P_2 persons (~ 20% of whites and ~ 80% of Asians)[6,10] express only P and low amounts of P^k. However, rare phenotypes exist, having anomalies in one or more of the P/P1/P^k blood group antigens. Individuals deficient in P antigen have mutations in the *B3GALNT1* gene causing lack of functional P (Gb_4) synthase (β3GalNAc transferase)[9,11] and consequently express increased levels of precursor, P^k. These persons may express P_1 antigen (P_1^k phenotype) or not (P_2^k), but the molecular basis for this is still unclear.[10] Persons without any P/P1/P^k antigens have mutations in the *A4GALT* gene (α4Gal transferase or P^k (Gb_3) synthase), causing lack of P^k synthesis, and the rare p blood group phenotype.[11-14] (Table 1).

The P and P^k antigens are glycosphingolipids (GSLs), and GSLs play an important role in HIV-host cell interactions.[15-18] HIV envelope glycoprotein gp120 targets CD4 and CCR5 or CXCR4 chemokine coreceptors on monocytes and T cells, as the major HIV-host cell interaction,[19-21] but HIV gp120 also binds to several GSLs in vitro, including P^k.[15-17,22] GSL interactions are mediated by a sphingolipid recognition motif on the gp120-V3 loop, thought to facilitate post-CD4 binding and membrane fusion.[18,22] Inhibition of GSL biosynthesis can prevent HIV-host cell membrane fusion and infection.[23,24] This can be overcome by reintroduction of purified GSLs, or overexpression of CD4 and CXCR4, suggesting that GSLs have a facilitative role.[24] P^k, and to a lesser extent GM3, has appeared to be primarily implicated in augmenting HIV-membrane fusion, at least in in vitro reconstitution models.[24]

Submitted March 14, 2008; accepted December 11, 2008. Prepublished online as *Blood* First Edition paper, January 12, 2009; DOI 10.1182/blood-2008-03-143396.

An Inside *Blood* analysis of this article appears at the front of this issue.

The publication costs of this article were defrayed in part by page charge payment. Therefore, and solely to indicate this fact, this article is hereby marked "advertisement" in accordance with 18 USC section 1734.

Table 1. P/GLOB-related* blood group phenotypes and frequencies

Phenotype	Antigen present on red blood cells	Frequency of red blood cell phenotype†
P_1	P1, P^k, P	75%–80%
P_2	P^k, P	20%–25%
p	None	~ 5 per 10^6
P_1^k	P1, P^k	~ 1 per 10^6
P_2^k	P^k	~ 1 per 10^6

*According to the International Society of Blood Transfusion working party on terminology of red cell–surface antigens, the P blood group system only contains the P1 antigen, whereas the GLOB blood group system includes the P antigen. The remaining related antigens (P^k and LKE, not mentioned here) are part of the GLOB blood group collection.

†Phenotypic frequencies are for whites.

In contrast, our recent work suggested P^k, when accumulated because of a lack of activity of α-galactosidase A in Fabry disease,[25] is protective against R5 HIV-1.[26] In addition, a soluble analog of P^k inhibits HIV infection in vitro.[27] Moreover, HIV-infected peripheral blood–derived mononuclear cells (PBMCs) have increased GSL expression, including P^k, indicating a potential cellular response to HIV-1.[28] Recently, pharmacologic modulation of P^k expression in vitro in HIV-1–infectable P^k-expressing non-T cells has further implicated an important role for P^k in HIV infection.[29]

In light of these findings, we have now assessed HIV-1 susceptibility of PBMCs that are naturally high in P^k (P_1^k phenotype) or naturally devoid of P^k (p phenotype). In addition, we have genetically and biochemically manipulated P^k expression in HIV-1–infectable $CD4^+$ HeLa cells and Jurkat T cells. Our findings show significant differences that reveal P^k status to be an important factor for susceptibility to HIV-1 infection.

Methods

Cells and chemicals

Waste buffy coat material from anonymous regular blood donors was from the Lund University Hospital Blood Center (Lund, Sweden). This provision complies with current national regulation regarding the use of superfluous material from blood donations where the donor origin cannot be traced. Consent was obtained at the time of donation. Waste buffy coat material was provided from various centers with informed consent according to the Declaration of Helsinki from the donors of P_1^k and p phenotype blood and made anonymous for this study. The protocol was reviewed and approved by the Canadian Blood Services Institutional Review Board Committee. The regular donor controls were matched for ABO group and date of donation. PBMCs and lymphoblastic cell lines were cultured in "complete medium" consisting of RPMI 1640 medium (Invitrogen, Burlington, ON) plus 10% fetal bovine serum, 2 mM L-glutamine, and 10 μM gentamicin antibiotics. The human T-cell line, Jurkat FHCRC (Jurkat C), was a gift from Dr Gordon Mills (M. D. Anderson Cancer Center, Houston, TX), and Jurkat E6.1 and MT-4 cells were obtained from the National Institutes of Health (NIH) AIDS Research and Reference Reagent Program (Rockville, MD). The human cervical cancer cell line, HeLa (clones 6C [HT4-6C] and 1022), stably transfected to express CD4 ($CD4^+$ HeLa) and sorted for high expression for infection with HIV-1, was obtained from the NIH AIDS Research and Reference Reagent Program or from Dr Alan Cochrane (University of Toronto, Toronto, ON) and cultured in RPMI plus 10% fetal bovine serum, 0.01% gentamicin antibiotics, and 0.1% amphotericin B. Test and control blood was collected into acid-citrate-dextrose anticoagulant on the same day and transported together to Canada for analyses. On arrival, PBMCs were isolated and activated using phytohemagglutinin (PHA)/interleukin-2 (IL-2) or PHA alone as described.[26] D-threo-1-phenyl-2-palmitoylamino-3-pyrrolidino-1-propanol (P4) was purchased from Matreya (Pleasant Gap, PA).

Blood group characterization

Blood samples acquired for this study were characterized extensively for categorization as control (P_1 or P_2), p, or P_1^k. Standard serologic techniques determined the erythrocyte phenotype and antibody specificities of blood samples. DNA was isolated from whole blood with the Qiagen QIAmp Blood Extraction kit (QIAGEN, Hilden, Germany). Genotypic characterization of samples was performed as reported.[9,14] (Tables 2, 3).

Viruses and in vitro infections

X4 HIV-1_{IIIB} and R5 HIV-$1_{Ba\text{-}L}$ were from the National Institutes of Health AIDS Research and Reference Reagent Program, Division of AIDS, National Institute of Allergy and Infectious Diseases, NIH: $HTLV_{IIIB}$ = HIV-1_{IIIB} from Dr Robert Gallo, HIV-$1_{Ba\text{-}L}$ from Dr Suzanne Gartner, HIV-$1_{JR\text{-}FL}$ from Dr Irvin Chen, HIV-$1_{Ada\text{-}M}$ from Dr Howard Gendelman, and HIV-$1_{NL4\text{-}3gp41(36G)\ V38E,\ N42S}$ from Trimeris (Durham, NC). HIV-1_{IIIB} viral stocks were grown in Jurkat C cells, and multiplicity of infection (MOI) was determined as described using MT-4 cells.[30] All other viral stocks were grown in PBMCs, and infectious dose calculated from total $p24^{gag}$ levels[31,32] measured by enzyme-linked immunosorbant assay (ELISA; Beckman Coulter, Fullerton, CA or ZeptoMetrix, Buffalo, NY). Briefly, cells were incubated with HIV-1 for 1 hour at 37°C, the cells washed extensively with phosphate-buffered saline (PBS), and cultured in complete medium. Culture supernatant aliquots were taken 2 hours after initial viral infection and subsequent time points. To determine viral production, ELISA was used to measure $p24^{gag}$ antigen levels.

FACS analysis

Fluorescence-activated cell sorter (FACS) analysis was performed as previously described using PHA- and PHA/IL-2–activated PBMCs and 1.5 μg monoclonal mouse anti-GM3 or anti-P^k (both from Seikagaku, Tokyo, Japan).[26] Alternatively, 12.5 μg/mL monoclonal mouse anti-CCR5 (clone 45549.111; NIH AIDS Research and Reference Reagent Program) was used. Secondary antibodies were either 5 μg/mL allophycocyanin (APC)–labeled goat antimouse IgG (Invitrogen) or 1 μL fluorescein isothiocyanate (FITC)–labeled goat antimouse IgG (Sigma-Aldrich, St Louis, MO). For anti-GM3–labeled samples, 10 μg/mL APC-labeled goat anti–mouse IgM was used (Cedarlane Laboratories, Burlington, ON).

Table 2. Summary of the P/GLOB-related blood group genetic and serologic findings in the rare persons whose cells were used in this study

Sample ID in this study	Genetic change		Cellular antigens*			Antibodies in serum†	Phenotype	Original description of the allele causing phenotype
	A4GALT	*B3GALNT1*	P1	P	P^k			
p1	657delG	No change	−	−	−	P, P1, P^k	P	Hellberg et al[14] (2003)
p2	548T>A	No change	−	−	−	P, P1, P^k	P	Steffensen et al[13] (2000)
p3	548T>A	No change	−	−	−	P, P1, P^k	P	Steffensen et al[13] (2000)
P_1^k-a	No change	811G>A	+	−	+	P	P_1^k	Hellberg et al[9] (2002)
P_1^k-b	No change	538insA	+	−	+	P	P_1^k	Hellberg et al[9] (2002)

+ indicates present; and −, absent.

*The P1 antigen is present in P_1 and P_1^k phenotype samples, detectable with anti-P1 but absent in P_2 and P_2^k and p.

†Anti-PP1P^k is also known as anti-Tj^a and is only found in individuals having the p phenotype.

Table 3. Summary of the P/GLOB-related blood group genetic and serologic findings in the control persons whose cells were used in this study

Sample ID in this study	Genetic change		Cellular antigens			Antibodies in serum	Phenotype
	A4GALT	*B3GALNT1*	P_1	P	P^k*		
Control a (C-a)	−	−	+	+	±	None	P_1
Control b (C-b)	−	−	+	+	±	None	P_1
Control p1 (C-p1)	−	−	+	+	±	None	P_1
Control p2 (C-p2)	−	−	+	+	±	None	P_1
Control p3 (C-p3)	−	−	+	+	±	None	P_1

*All blood group phenotypes with the exception of p, P_1^k, and P_2^k express low levels of P^k because of incomplete conversion to P. The amount of P^k expressed varies from person to person.

FACS analysis for P^k expression of small interfering (si)RNA-transfected $CD4^+$ HeLa cells was carried out using 5 μg/mL VT1B-$Alexa_{458}$ (produced in the Lingwood laboratory). For tricolor FACS analysis, an additional incubation with 20 μL 10% mouse serum in FACS buffer for 10 minutes at 4°C in the dark was carried out before incubation with 10 μL mouse anti–CD4-peridinin chlorophyll protein (PerCP) Cy5.5 (BD Biosciences, San Jose, CA) and/or 5 μL mouse anti–CXCR4-phycoerythrin (PE; Serotec, Oxford, United Kingdom). Data were collected with a calibrated (BD CaliBRITE; BD Biosciences) Becton Dickinson FACSCalibur cell cytometer and analyzed using CellQuest software.

TLC of GSLs

Extraction and thin layer chromatography (TLC) separation of GSLs, including ganglioside GM3, was as previously described.[33] GSL species were detected either by orcinol spray (Sigma-Aldrich) at 110°C for 10 minutes, or P^k selectively detected by verotoxin-1 (VT1) TLC overlay.[34] For VT1 overlay, the plate was blocked with 1% bovine gelatin; and after incubation at 37°C, the plate was washed with 50 mM Tris-buffered saline (TBS), pH 7.4. The plate was incubated for 45 minutes at room temperature with purified VT1, 1 μg per 10 mL in TBS. After washing, the plate was incubated for 45 minutes with a monoclonal antiverotoxin B subunit[34] (diluted 1/2000), washed and incubated with horseradish peroxidase-conjugated goat antimouse IgG (diluted 1/2000; Bio-Rad, Hercules, CA). For GM3 immunostaining, monoclonal anti-GM3 was substituted for VT1, followed by incubation with horseradish peroxidase–conjugated goat antimouse IgG. The plate was developed for 1 to 10 minutes with a 3 mg/mL solution of 4-chloro-1-naphthol in methanol freshly mixed with 5 volumes of TBS and 1/2000 dilution of 30% H_2O_2. Where band intensity was calculated from TLC blots, ImageJ software (NIH) was used to quantify relative intensities of bands visualized on TLC, where background signals were subtracted.

Liposome fusion of Jurkat E6.1 cells

Jurkat E6.1 cells do not express P^k and are highly infectable with HIV-1. P^k or P liposomes were prepared by drying 400 μg P^k or P (Sigma-Aldrich) with 200 μg phosphatidylethanolamine and 200 μg phosphatidylserine in chloroform/methanol (2:1) under nitrogen. Alternatively, control phospholipid (PL) liposomes were prepared by drying 200 μg phosphatidylethanolamine with 200 μg phosphatidylserine. Liposomes were generated by vortexing well in 400 μL PBS and sonicating for 30 minutes. Liposomes or equivalent volumes of PBS were incubated with 16×10^6 Jurkat E6.1 cells (4×10^6 cells/mL) in serum-free RPMI 1640 for 1 hour at 37°C on a shaker (100 rpm). After incubation, cells were washed twice with PBS and cultured 18 to 24 hours at 37°C before infection with $HIV\text{-}1_{IIIB}$.

Adenoviral vector production

Ad5/F35 vectors were generated as previously described[35] by in vivo recombination in *Escherichia coli* BJ5183 cells between pAdenoVator transfer plasmids and pAdEasy-1/F35 adenoviral genome (a generous gift from Dr X. Fan, Lund University, Lund, Sweden)[36] using the AdenoVator Vector system (Qbiogene, Irvine, CA). Transfer plasmids containing the cytomegalovirus (CMV) promoter/enhancer with a β-globin/IgG chimeric intron (CMVi) were purchased from Qbiogene. For enhanced yellow fluorescent protein (EYFP) control Ad5/F35 vectors, EYFP from pIRES-EYFP (Clontech, Mountain View, CA) was cloned into the transfer plasmids. For P^k expression, Ad5/F35 vectors containing an expression cassette encoding EYFP under the control of the mouse PGK promoter[35] was first cloned into the CMVi transfer plasmid, and the full-length human P^k synthase (P^k-S) cDNA, cloned from CaCo-2 cells using primers for reverse-transcribed polymerase chain reaction that were designed based on the published sequence (GenBank database accession no. AB037883),[37] was then cloned into the CMVi expression cassette.

Recombinant Ad5/F35 vectors were transfected into QBI-293A cells using a standard calcium phosphate transfection procedure, and recombinant viruses were plaque-purified. Viruses were than amplified by transduction of large HEK293 cell cultures. Viruses were extracted by 3 consecutive freeze-thaw cycles and purified by a discontinuous CsCl gradient followed by a continuous CsCl gradient to completely separate infectious from defective viral particles. The viral preparations were dialysed against Tris 20 mM, pH 8, 2.5% glycerol, and 25 mM NaCl, concentrated using Amicon Ultra-4 MWCO 30 000 concentrators (Millipore, Ville St Laurent, QC) and sterilized by filtration through 0.22 μm Millex-GV filters (Millipore). The viral titers were determined by the tissue-culture infectious dose ($TCID_{50}$) method following the manufacturer's instructions (Qbiogene). Two adenoviral vectors were made: a control vector (pAd5/F35-CMVi-EYFP) and a test vector (Ad5/F35-CMVi-P^k-S-EYFP). The titers of the viral stocks were between 3×10^8 and 1×10^9 infectious units/μL.

P^k-synthase gene transduction

Approximately 5×10^5 $CD4^+$ HeLa cells were plated in triplicate in 6-well plates and incubated overnight. Cells were then incubated for 1 hour at 37°C and 5% CO_2 in 250 μL Iscove modified Dulbecco medium (IMDM) containing the control (pAd5/F35-CMVi-EYFP) or test (Ad5/F35-CMVi-P^k-S-EYFP) vector at a MOI of 25. Untransduced control cells received 250 μL of IMDM only. After incubation, IMDM media was added to a volume of 2 mL. Plates were incubated at 37°C and 10% CO_2 for 48 hours; and after transduction, cells were recovered and subjected to FACS analysis and infection with X4 $HIV\text{-}1_{IIIB}$ (MOI, 0.3) where productive infection was monitored over time.

Depletion of glucosyl ceramide-based GSLs

The glucosyl ceramide synthase inhibitor, P4,[38] was used at 2 μM to pretreat $CD4^+$ HeLa cells for 5 days before HIV infection. FACS analysis indicated that this treatment was sufficient to greatly reduce cell-surface expression of P^k without cell toxicity.[29] After 5 days of P4 treatment, cells were washed and then infected with X4 $HIV\text{-}1_{IIIB}$ (MOI, 0.3) and productive infection monitored over time.

Transient siRNA depletion of P^k synthase gene expression

Approximately 2×10^5 $CD4^+$ HeLa cells were plated in triplicate in 6-well plates and incubated overnight in antibiotic-free RPMI media. Media was then replaced with serum-free, antibiotic-free RPMI. Depletion of P^k-S by siRNA was carried out as per the manufacturer's instructions (Thermo Electron, Waltham, MA) with modifications. Briefly, 2 μL Dharmafect-1 was added to 198 μL serum-free RPMI (tube 1). At the same time, 100 μL siRNA (2μM) was added to 100 μL serum-free RPMI (tube 2). Both tubes were mixed separately by pipetting and incubated for 5 minutes. Tube 1 was then added to tube 2, mixed

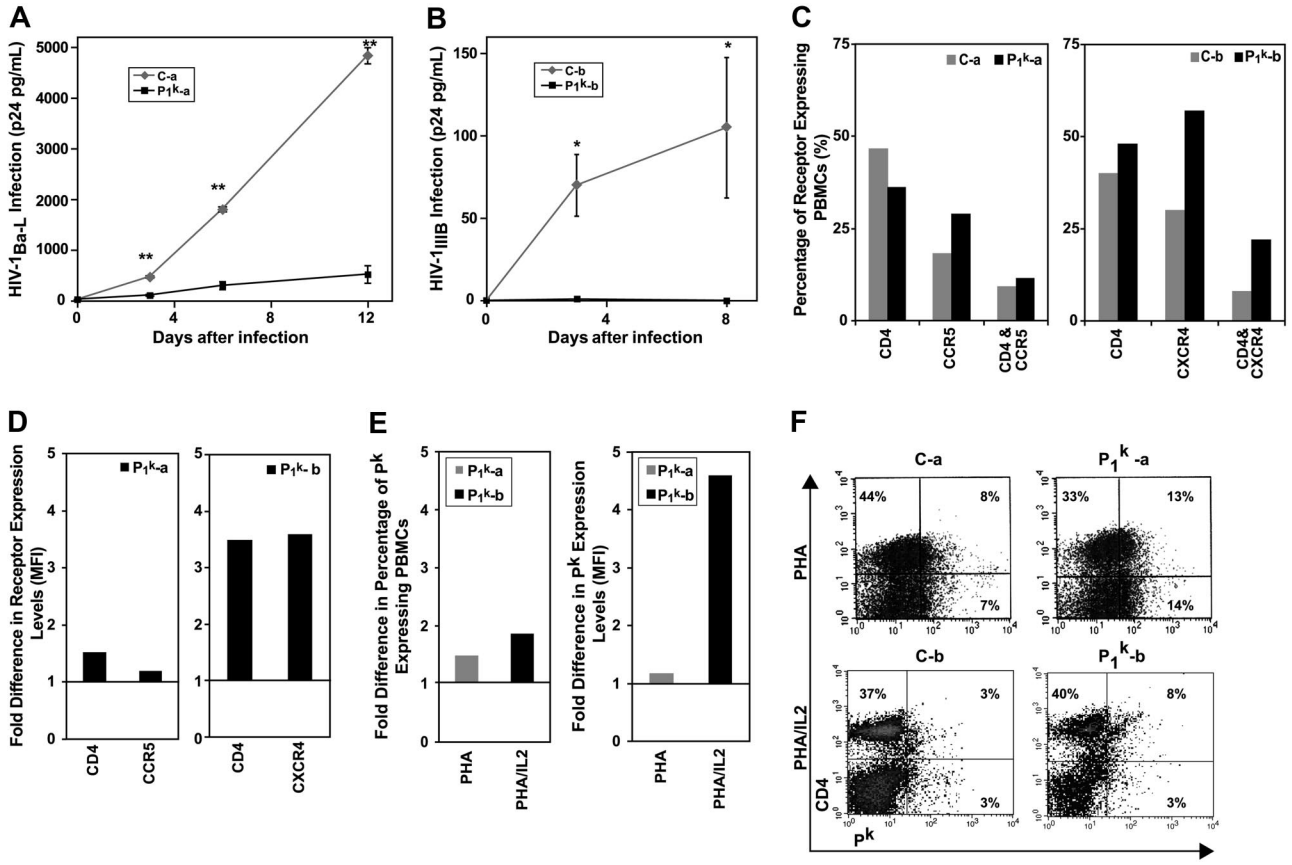

Figure 1. Decreased susceptibility of P_1^k PBMCs to R5 and X4 HIV-1 infection inversely correlates with P^k and does not correlate with CD4 and/or chemokine coreceptor expression. (A) PHA-activated PBMCs were infected with HIV-$1_{Ba\text{-}L}$ (0.5 ng HIV $p24^{gag}$/5 × 10^5 cells) and (B) PHA/IL-2–activated PBMCs were infected with HIV-1_{IIIB} (MOI, 0.3). Viral propagation was monitored by $p24^{gag}$ antigen up to 12 days and plotted as a function of time: (A) $^{**}P < .002$. (B) $^{*}P < .05$. Data are representative of the mean plus or minus SEM, where n = 4 infection data points. (C-F) Scatter plots of PBMCs labeled with anti–CD4 PerCP Cy5.5, anti–CCR5 GAM-FITC (or GAM-APC), and anti–CXCR4-PE were analyzed, and background compensated to isotype controls. Alternatively, anti–CD4 PerCP Cy5.5 and anti-P^k GAM-APC were used to label PBMCs and analyzed as described. (C) Percentage of cell populations expressing CD4, CCR5, and CXCR4, present in PHA-activated (left) or PHA/IL-2 activated PBMCs (right) plotted as histograms for ease of comparison. (D) MFI of surface expressed CD4, CCR5, and CXCR4 was measured on ungated cell populations and fold difference in expression levels calculated based on control MFI values for PHA-activated PBMCs (left) or PHA/IL-2–activated PBMCs (right). (E) Percentage of P_1^k-PBMC cell populations expressing surface P^k (left) and P^k expression levels based on MFI (right) are represented as fold difference based on control values. (F) Scatter plots representing CD4 and P^k expressing cell populations. (Top panel) PHA-activated PBMCs. (Bottom panel) PHA/IL-2-activated PBMCs. Left: Control PBMCs. Right: P_1^k PBMCs. ◇ or □ represent healthy PBMCs controls designated C-a or C-b (Table 3); (■), P_1^k = P_1^k PBMCs designated P_1^k-a or P_1^k-b (Table 2).

carefully, and incubated for 20 minutes at room temperature. This mixture was added to cells, which were subsequently cultured for 24 hours. This procedure was repeated after 24 and 48 hours. The siRNA depletion of P^k-S was monitored by FACS analysis of P^k expression. $CD4^+$ HeLa cells, with demonstrated reduction in surface levels of P^k (> 70%), were infected with X4 HIV-1_{IIIB} (MOI, 0.3) and aliquots of culture supernatant taken over time to monitor $p24^{gag}$ production by ELISA.

Statistics

A 2-sample Student *t* test, assuming unequal variance with 2-tailed distribution, was used to determine significance. The means of the data points for blood group phenotype were compared with their respective matched controls and represented plus or minus SEM, where n = 4. The means of the data points for treated/manipulated cells were compared with their respective control-treated or unmanipulated cells and represented plus or minus SEM, where n = 3 or 4. Data were considered statistically significant if *P* was less than .05 or highly significant if *P* was less than .002.

Results

P_1^k PBMCs are protected against R5 and X4 HIV-1 infection

We first assessed the susceptibility to HIV-1 infection of PBMCs from P_1^k persons. Given the rarity of these samples (Table 1),[6] P_1^k PBMCs from one donor (P_1^k-a) were used to assess R5 HIV-1 infection and a second donor (P_1^k-b) to assess X4 HIV-1 infection (Tables 2 and 3 for test and control designations, respectively). Infection of PHA-activated P_1^k-a with R5 HIV-$1_{Ba\text{-}L}$ showed significantly lower productive HIV-$1_{Ba\text{-}L}$ infection compared with its draw-date- and ABO-matched control (Figure 1A). PHA/IL-2–activated P_1^k-b were similarly protected against productive X4 HIV-1_{IIIB} infection (Figure 1B) compared with the respective control. Based on comparison with draw-date–matched controls, infection levels for P_1^k PBMCs for both HIV-$1_{Ba\text{-}L}$ and HIV-1_{IIIB} were less than 12% (data not shown).

CD4, coreceptor, and P^k expression are increased in P_1^k PBMCs

To determine whether expression levels of HIV receptors may have influenced the reduced infection levels, cell-surface CD4, CCR5, and CXCR4 levels on the same cell populations used for infection studies were analyzed by flow cytometry. PHA-activated P_1^k-a showed approximately 10% less CD4-expressing cells than the matched control; however, CD4 expression levels (mean fluorescence intensity [MFI]) were approximately 1.5-fold higher (Figure 1C,D left panels). There were also approximately 11% more

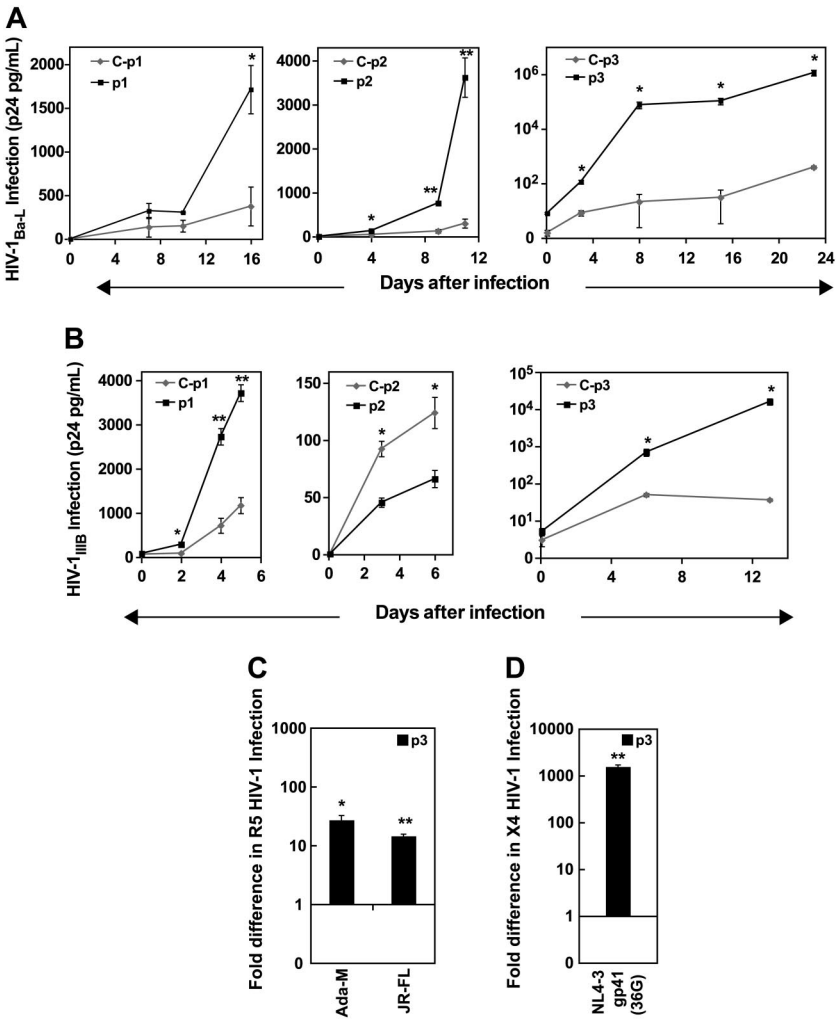

Figure 2. Increased susceptibility of p PBMCs to R5 and X4 HIV-1 infection. PHA-activated PBMCs or PHA/IL-2–activated PBMCs were infected with R5 or X4 HIV-1 strains. HIV-1 propagation was monitored by $p24^{gag}$ antigen up to 25 days after infection, and plotted as a function of time. (A) R5 HIV-$1_{Ba\text{-}L}$ (0.5 ng HIV $p24^{gag}/5 \times 10^5$ cells). (B) X4 HIV-1_{IIIB} (MOI, 0.3). (C) R5 HIV-$1_{Ada\text{-}M}$ (13.3ng of HIV $p24^{gag}/5 \times 10^5$ cells), R5 HIV-$1_{JR\text{-}FL}$ (3.25 ng HIV $p24^{gag}/5 \times 10^5$ cells). (D) X4 HIV-$1_{NL4\text{-}3\ gp41\ 36G}$ (11.6 ng HIV $p24^{gag}/5 \times 10^5$ cells). (C,D) Fold change was calculated for each p donor (p1, p2, and p3) based on control infection levels of samples taken at the last time point. Data are representative of the mean ± SEM, where n = 4 infection data points, $^*P < .05$, $^{**}P < .002$. ◇ represents healthy PBMCs controls designated C-p1, C-p2, or C-p3 (Table 3); (■), p PBMCs designated p1, p2, or p3 (Table 2).

CCR5-expressing cells in P_1^k-a and slightly higher CCR5 expression (MFI ~ 1.2-fold difference; Figure 1C,D). The percentage of R5 HIV-1–susceptible target PBMCs, expressing both CD4 and CCR5, was also slightly higher in P_1^k-a (Figure 1C).

PHA/IL-2–activated P_1^k-b demonstrated approximately 7% more CD4-expressing cells compared with control and approximately 3.5-fold higher CD4 expression levels (MFI) (Figure 1C,D right panel). In addition, there were 27% more CXCR4-expressing cells than control, and approximately 3.5-fold higher CXCR4 expression in P_1^k-b (Figure 1C,D). Indeed, even the percentage of X4 HIV-1–susceptible target PBMCs, expressing both CD4 and CXCR4, was higher in P_1^k-b (Figure 1C). The percentage of cells expressing cell-surface P^k on PHA- and PHA/IL-2-activated P_1^k PBMCs was approximately 1.5- to 2-fold higher than that of controls (Figure 1E), with up to 4.5-fold higher density of cell-surface P^k expression as measured by MFI (Figure 1E). Cells expressing both CD4 and P^k, which encompass HIV-1–susceptible target cells, were also found to be twice as frequent in P_1^k PBMCs compared with their respective controls (Figure 1F).

p PBMCs are hypersusceptible to R5 and X4 HIV-1 infection

We also assessed susceptibility of PBMCs from 3 P^k-deficient p persons (Table 2) to R5 and X4 HIV-1 infection. HIV-$1_{Ba\text{-}L}$ infection of PHA-activated p PBMCs (denoted p1, p2, and p3; Table 2) resulted in much higher levels of productive infection compared with their drawdate- and ABO-matched control (Figure 2A). Following infection over time depicts exponential kinetics in HIV-1 production for p PBMCs. The difference in infection levels between p PBMCs and control showed a change of approximately 5-fold higher for p1, 12-fold higher for p2, and approximately 3000-fold higher for p3 (data not shown). This increased infection was consistent for R5 HIV-1 infection in general, as 2 other R5 strains, HIV-$1_{Ada\text{-}M}$ and HIV-$1_{JR\text{-}FL}$, also showed much higher productive HIV-1 infection in the p PBMCs compared with control (Figure 2C).

As with R5 infection, HIV-1_{IIIB} infection of PHA/IL-2-activated p PBMCs from 2 persons (p1 and p3) also showed much higher levels of productive infection compared with their matched controls (Figure 2B,D). However, the p2 sample showed a 2-fold lower infection level (Figure 2B center panel), but overall infection in this experiment (C-p2 and p2) was much less than for the other p PBMC experiments. For the last p1 and p3 samples analyzed, the difference in infection levels between p PBMCs and their respective controls showed a change of 3-fold higher for p1 and approximately 600- to 1000-fold higher for p3 (Figure 2B). One other X4 strain, HIV-$1_{NL4\text{-}3\ gp41}$, used to infect PHA/IL-2-activated p3 also showed more than 1000-fold higher productive HIV-1 infection compared with control (Figure 2D), consistent with X4 HIV-1_{IIIB} results.

CD4 and coreceptor expression are increased in p PBMCs

To determine whether expression levels of HIV receptors influenced the observed susceptibility to infection, the same cell

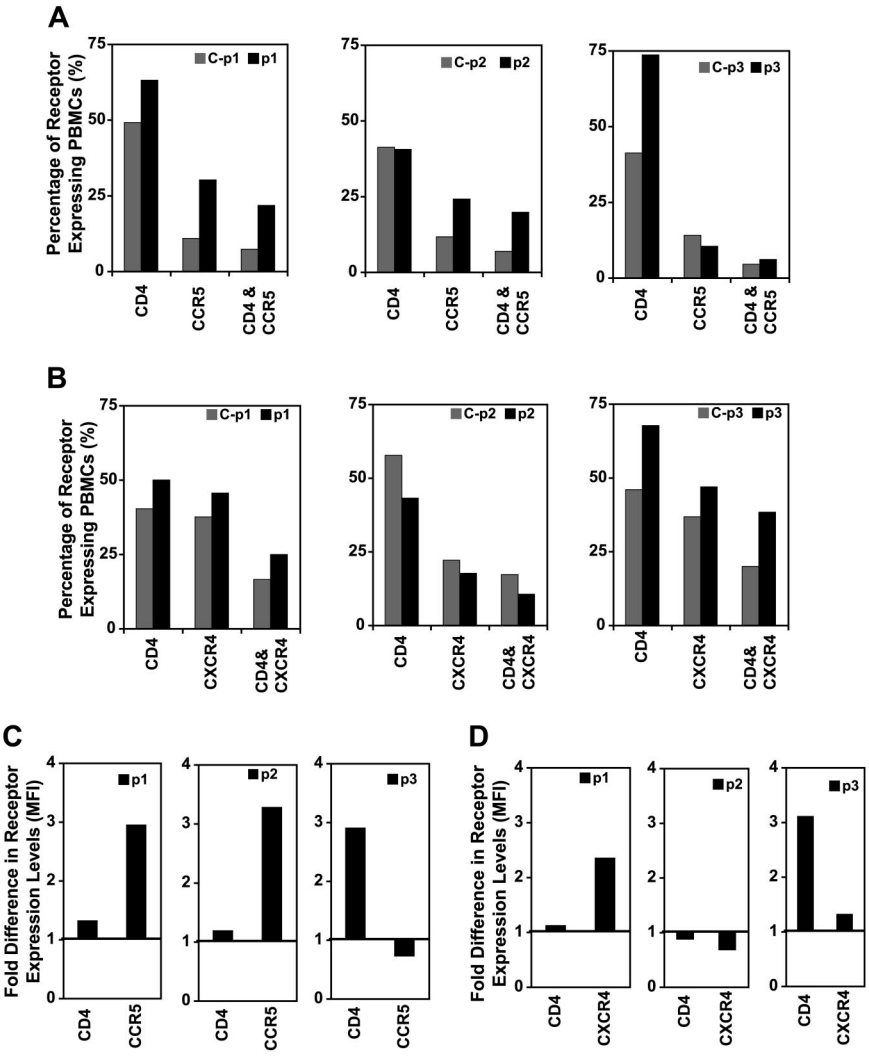

Figure 3. FACS analysis of CD4, CCR5, and CXCR4 expression on p PBMCs. PBMCs were either stimulated with PHA or PHA/IL-2 (as per conditions for HIV infection) and tricolor FACS analysis was performed. Scatter plots of PBMCs labeled with anti-CD4 PerCP Cy5.5, anti–CCR5 GAM-FITC (or GAM-APC), and anti–CXCR4-PE were analyzed, and background compensated to isotype controls. (A,B) Percentage of cell populations expressing CD4, CCR5, and CXCR4, present in PHA-activated PBMCs (A) or PHA/IL-2-activated PBMCs (B) plotted as histograms for ease of comparison. (C,D) MFI of surface expressed CD4, CCR5, and CXCR4 was measured and fold difference in expression levels calculated based on control values for PHA-activated PBMCs (C) or PHA/IL-2–activated PBMCs (D). ■ represents healthy PBMC controls designated C-p1, C-p2, or C-p3 (Table 3); ■, p PBMCs designated p1, p2, or p3 (Table 2).

population used for infection was subjected to flow cytometry to determine cell-surface CD4, CCR5, and CXCR4. In general, PHA-activated p PBMCs (p1, p3) presented more CD4-expressing cells than their controls (an increase of ~ 14%-40%), which also translated into higher CD4 expression levels (MFI, 1.3- to 3-fold higher; Figure 3A,C). This was most evident for p3, which showed the highest susceptibility to R5 HIV-1. There were also more CCR5-expressing cells in p PBMCs (p1, p2; an increase of ~ 12%-19%), and 3-fold higher CCR5 expression levels (MFI; Figure 3A,C). Furthermore, the percentage of R5 HIV-1–susceptible target PBMCs, expressing both CD4 and CCR5, was greater in p PBMCs (p1, p2, and slightly in p3; Figure 3A). However, p3 PBMCs showed reduced CCR5 levels (Figure 3A,C).

PHA/IL-2–activated p PBMCs (p1, p3) demonstrated more CD4-expressing cells compared with their controls (an increase of ~ 21%-42%), and up to 3-fold higher CD4 expression levels (MFI; Figure 3B,D). These differences were once again most evident in p3, which demonstrated the highest increase in X4 HIV-1 infection. The p3 sample showed more CXCR4-expressing cells than control (> 10%), and overall there was 1.3- to 2.3-fold higher CXCR4 expression in p-PBMCs from both p1 and p3 samples (Figure 3B,D). The percentage of X4 HIV-1–susceptible target PBMCs, expressing both CD4 and CXCR4, was noticeably higher in p PBMCs from p3 (Figure 3B). In contrast, p2 showed a somewhat opposite expression profile, exhibiting approximately 15% less CD4 and approximately 5% less CXCR4 expressing cells compared with the matched control (Figure 3B center panel), as well as lower receptor expression levels (MFI; Figure 3D center panel).

GM3 expression in p PBMCs does not account for increased infection

Increased HIV-1–induced T-cell fusion has been reported in p-CD4$^+$ T cells, ascribed to higher total levels of GM3.[39] Although GM3 is reported less fusogenic than Pᵏ,[24], we investigated the possibility that GM3 levels influenced p-PBMC (p3) susceptibility to infection in our system. Total GSLs isolated from PHA-activated PBMCs revealed loss of GM3 in control compared with p-PBMCs (Figure 4A), calculated according to band intensity on the TLC plate to be approximately 3-fold different (Figure 4C). Resting or PHA/IL-2–activated PBMCs, however, showed minimal differences in total p-PBMC GM3 levels compared with the respective control (Figure 4A-C). Higher total GM3 expression in PHA-activated p PBMCs did not translate to higher percentage of cells or cell-surface GM3 expression as measured by FACS analysis (Figure 4D center panel; Figure 4E). Although there was a slightly higher percentage of GM3-expressing p PBMCs in the PHA/IL-2–activated population, only subtle differences were seen in cell-surface GM3 expression (Figure 4D right panel; Figure 4E).

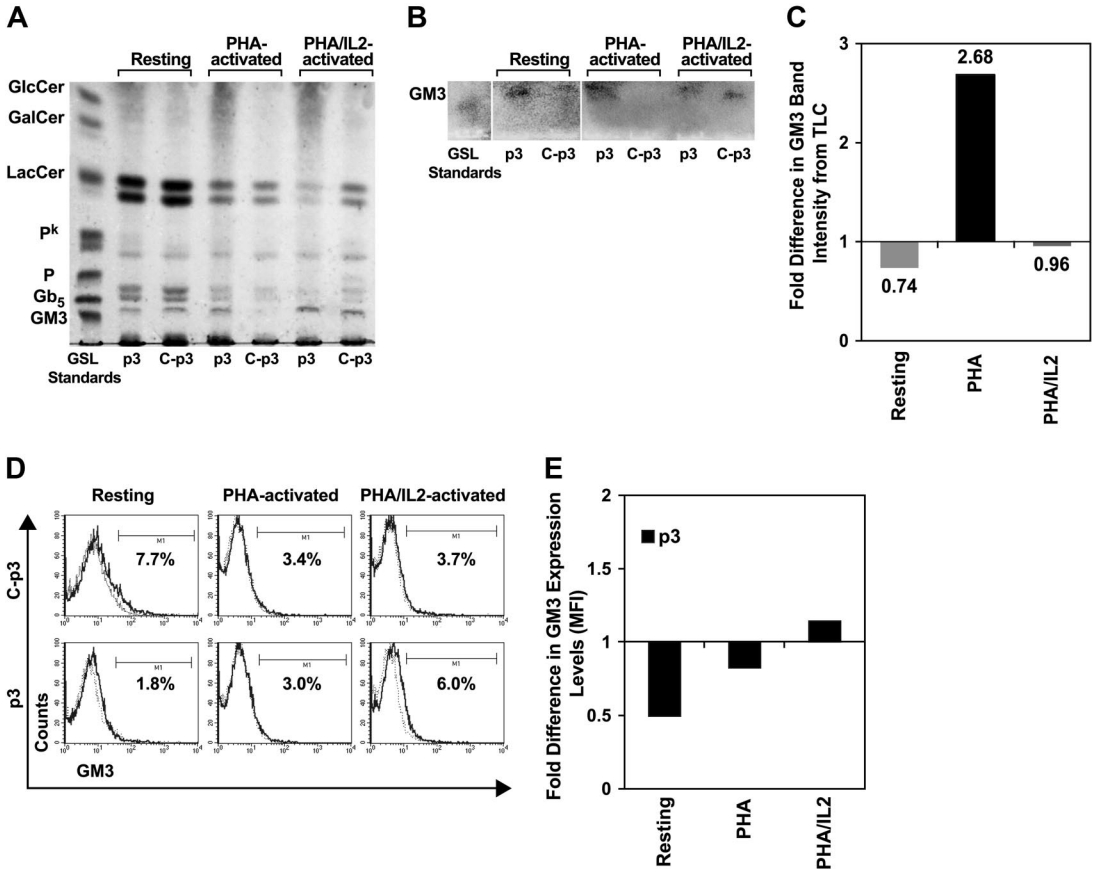

Figure 4. FACS and TLC of GM3 expression in p PBMCs. PBMCs were either resting or stimulated with PHA or PHA/IL-2 and analyzed for total and surface expressed GM3. (A,B) TLC of total GSLs extracted from control PBMCs (C; p3: lanes 3, 5, and 7) and p PBMCs (p3: lanes 2, 4, and 6). Lane 1: GSL standards. Lanes 2 and 3: Resting PBMCs. Lanes 4 and 5: PHA-activated PBMCs. Lanes 6 and 7: PHA/IL-2-activated PBMCs. (A) TLC of total GSLs. (B) TLC overlay to confirm the position of GM3. (C) Band intensity of GSLs represented on the TLC plate in panel B was measured by ImageJ software, compensated to background levels and fold difference in p-PBMC expression levels calculated based on control values. GlcC indicates glucosylceramide; GalC, galactosylceramide; LC, lactosylceramide; P^k, globotriosylceramide; P, globoside or globotetraosylceramide; Gb_5, globopentaosylceramide; GM3, ganglioside. (D) Histogram plots representing percentage of PBMCs labeled with anti-GM3 GAM-APC were analyzed, and background compensated to isotype controls. (Top panel) Control PBMCs (C-p3). (Bottom panel) p PBMCs (p3). (Left) Resting PBMCs. (Center) PHA-activated PBMCs. (Right) PHA/IL-2-activated PBMCs. (E) MFI of surface expressed GM3 was measured and fold difference calculated based on control values.

P^k-liposome fusion of Jurkat T cells decreases susceptibility to X4 HIV-1

Exogenous P^k was introduced into P^k-deficient Jurkat T-cell membranes by P^k-liposome fusion. After fusion, approximately 35% of the Jurkat cell population expressed surface P^k at high levels (MFI; Figure 5A,B). Within the $CD4^+$ target population, approximately 32% expressed both CXCR4 and P^k (Figure 5C right panel). P^k-liposome–treated cells showed no differences in CD4 or CXCR4 expression compared with PBS or PL-liposome controls (Figure 5B,C). Increased P^k expression after P^k-liposome transfer was confirmed by TLC (Figure 5E). A significant reduction in X4 HIV-1_{IIIB} infection was observed in the P^k supplemented Jurkat cells, being only 43% of the HIV-1_{IIIB} infection levels of PBS, P-, or PL-liposome controls (Figure 5F).

Increase in P^k synthase shows increased expression of P^k and decreased HIV-1 infection

To confirm that P^k expression levels influence HIV-1 infection levels, we tested whether modulating the expression of P^k in $CD4^+$ HeLa cells, which express P^k and are infectable, would correlate with subsequent HIV-1 infection (Figure 6). Cells transduced with adenoviral vector expressing P^k synthase (P^k-S) resulted in increased levels of total and cell surface P^k compared with nontransduced cells or cells transduced with a control adenoviral vector (Figure 6A,B). Compared with untreated cells or control adenoviral vector transduced cells, HIV-1 infection was significantly lower in the increased P^k-expressing $CD4^+$ HeLa cells transduced with the adenoviral vector P^k-S (Figure 6C).

Depletion of glucosyl ceramide–based GSLs, including P^k, shows increased HIV-1 infection

P4 was used to inhibit glucosylceramide-based GSL synthesis, thus blocking the biosynthetic pathway to P^k.[38] P4 treatment of $CD4^+$ HeLa cells resulted in a substantial decrease in cell populations expressing P^k (Figure 6D). A decrease in P^k expression was also shown in the total GSL profile (Figure 6E). P4-treated cells further demonstrated significantly increased HIV-1 infection levels (Figure 6F).

Transient siRNA depletion of P^k synthase reduced P^k expression and increased HIV-1 infection

To demonstrate that specific reduction of P^k influences the level of HIV-1 infection, siRNA was used to transiently silence the P^k synthase gene, encoding the enzyme responsible for the addition of the terminal galactose to the precursor for P^k.[5,10] Transfection of P^k synthase-specific siRNAs into $CD4^+$ HeLa cells resulted in a substantial decrease in cells expressing P^k compared with siRNA controls (Figure 7A,B). The decrease in total P^k was selective without significant decrease in P^k precursors GlcCer or LacCer, monitored by TLC and VT1 overlay (Figure 7B,C). Cells transiently transfected with siRNA to P^k synthase demonstrated significantly increased HIV-1 infection levels (Figure 7D).

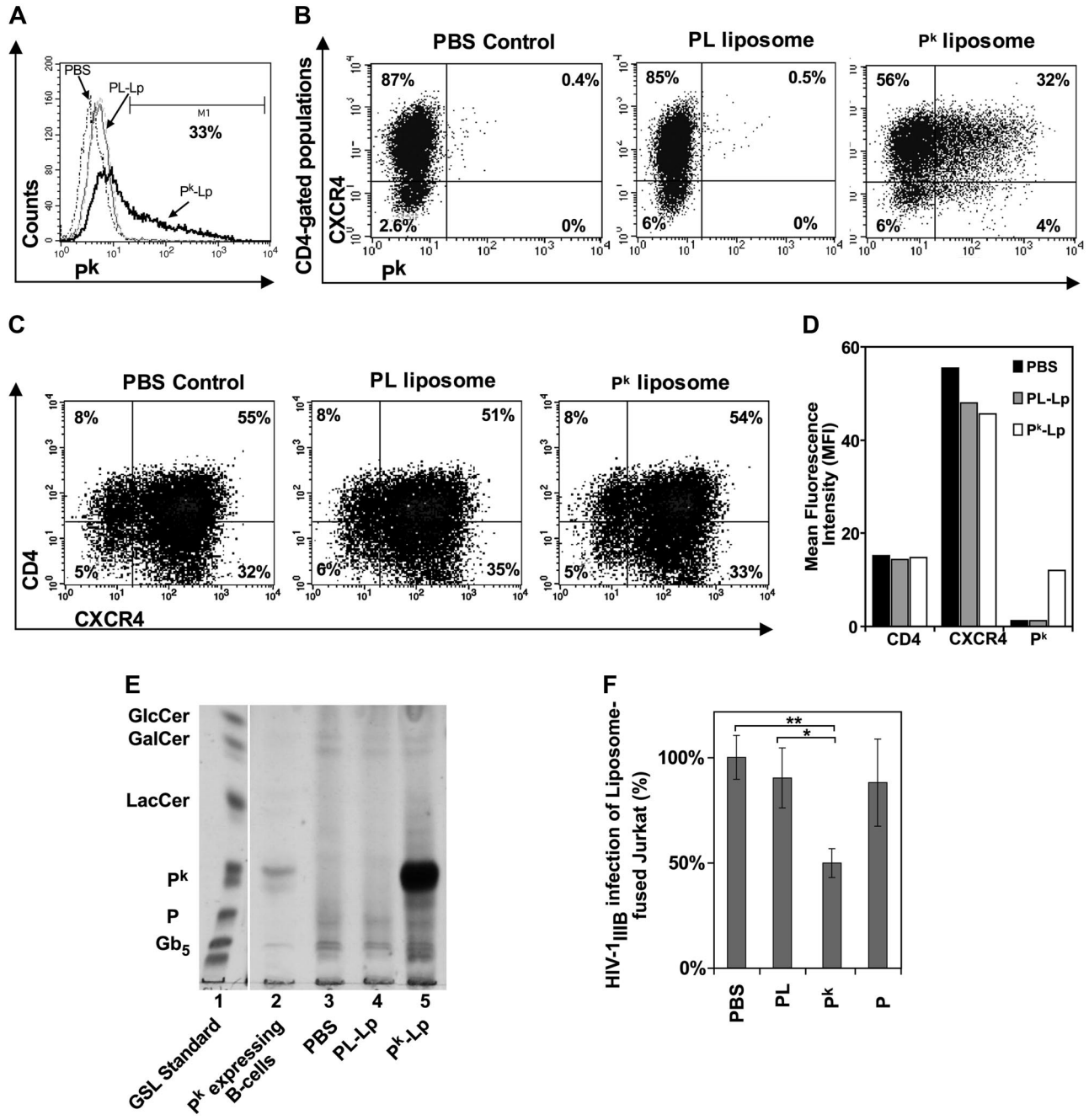

Figure 5. Susceptibility of Pᵏ-liposome–fused Jurkat T cells to X4 HIV-1 infection. Jurkat T cells lacking Pᵏ were incubated with Pᵏ- or P-liposomes and cultured for 18 hours, where PBS or PL-liposome controls were used. Tricolor FACS analysis was performed and scatter plots of Jurkat labeled with anti–CD4 PerCP Cy5.5, anti-CXCR4-PE, and anti–Pᵏ GAM-FITC (or GAM-APC) were analyzed, where background was compensated to isotype controls. (A) Histogram representing percentage of cell populations expressing Pᵏ. (B) Scatter plots representing cell populations expressing Pᵏ and CXCR4, and gated on CD4-positive populations. (Left) PBS-treated Jurkat. (Center) PL-liposome–fused Jurkat. (Right) Pᵏ-liposome–fused Jurkat. (C) Scatter plots representing percentage of cell populations expressing CD4 and CXCR4. (Left) PBS-treated Jurkat. (Center) PL-liposome–fused Jurkat. (Right) Pᵏ-liposome–fused Jurkat. (D) Surface expression levels of CD4, CXCR4, and Pᵏ are represented as MFI. (E) TLC of total GSLs extracted from control and liposome fused Jurkat cells. Lane 1: GSL standards. Lane 2: Pᵏ-expressing B-cell line control (Daudi). Lane 3: PBS-treated Jurkat control. Lane 4: PL-liposome control. Lane 5: Pᵏ-liposome–fused Jurkat. (F) Infection with HIV-1_{IIIB} (MOI, 0.3) and $p24^{gag}$ monitored at day 3 after infection (n = 3 or 4 infection data points). Percentage difference in infection was calculated based on PBS control infection levels, and data were pooled from 3 independent experiments to show significance between PL-liposome controls and Pᵏ-liposomes (*$P < .05$, **$P < .002$). PBS indicates PBS control; PL or PL-Lp, phospholipid liposome control; Pᵏ or Pᵏ-Lp, Pᵏ liposomes; P, P-liposomes.

Discussion

Our findings indicate a new phenomenon of Pᵏ-mediated reduced susceptibility to HIV-1 infection. $P_1{}^k$ PBMCs, which highly express Pᵏ on their cell surface, demonstrate lower levels of productive R5 and X4 HIV-1 infection. In contrast, p PBMCs, which do not express Pᵏ, show a higher susceptibility to R5 and X4 HIV-1 infection. Accordingly, Pᵏ-liposomal transfer or Pᵏ-synthase gene transduction facilitated a reduction in HIV-1 infection, whereas GlcCer-based GSL (Pᵏ) depletion or Pᵏ-synthase gene silencing resulted in an increase in HIV-1 infection. Thus, higher expression of Pᵏ in vivo and in vitro correlates with decreased HIV-1 infection, whereas a lower expression or lack of Pᵏ expression results in increased HIV-1 infection.

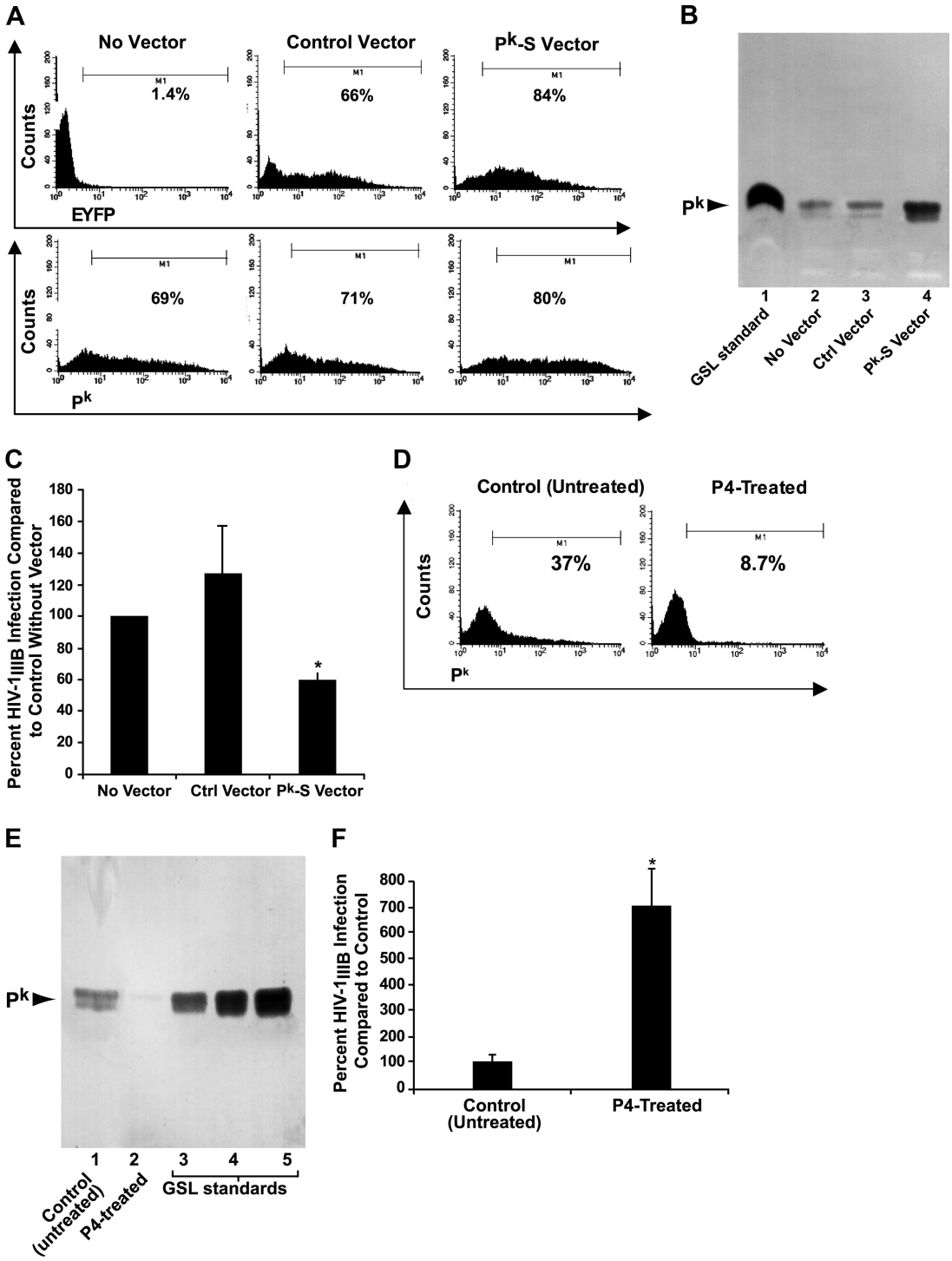

Figure 6. Molecular and chemical modulation of P^k expression. $CD4^+$ HeLa cells (clone 1022) were either untreated (no vector) or transduced with control adenoviral vector alone (control [Ctrl] vector) or adenoviral vector containing full-length human P^k synthase (P^k-S) cDNA (P^kS vector). Both the control and P^k-S vectors contained an EYFP gene to detect transduction efficiency. After 48 hours, FACS analysis was performed and scatter plots of $CD4^+$ HeLa cells labeled with anti–P^k GAM-FITC were analyzed, where background was compensated to isotype controls. (A) Histogram plots representing percentage of cell populations expressing EYFP (top panel) or P^k (lower panel) for no vector control (left), control vector (center), and P^k-S vector (right). (B) VT1 overlay for P^k detection was carried out on TLC of total GSLs extracted from control and transduced $CD4^+$ HeLa cells. Lane 1: GSL standards. Lane 2: Cells without adenovector (no vector). Lane 3: Cells with control adenovector (control vector). Lane 4: Cells with adenovector-expressing P^k synthase gene (P^k-S vector). (C) HIV-1_{IIIB} (MOI, 0.1) was used to infect $CD4^+$ HeLa cells with no vector, control vector, or P^k-S vector. After 3 days, HIV-1 infection was measured by $p24^{gag}$ production. Percentage difference in HIV-1 infection was calculated based on $CD4^+$ HeLa cells without adenovector (no vector). Data are representative of the mean plus or minus SEM where $n = 3$ infection data points; $^*P < .05$ comparing P^k-S–transduced cells to untransduced cells. This figure is representative of 3 independent experiments. (D) Histogram plots representing percentage of cell populations expressing P^k after $CD4^+$ HeLa cells (clone 6C) were either untreated (control) or treated with a GSL biosynthesis inhibitor (P4-treated, 2 μM) for 5 days to deplete glucosyl ceramide based GSLs, which includes P^k. (E) VT1 overlay for P^k detection was carried out on TLC of total GSLs extracted from untreated and P4-treated $CD4^+$ HeLa cells. Lane 1: Control (untreated) cells. Lane 2: P4-treated cells. Lane 3-5: GSL standards. (F) HIV-1_{IIIB} (MOI, 0.1) infection of untreated or P4-treated $CD4^+$ HeLa cells was measured by $p24^{gag}$ production after 3 days of culture. Percentage difference in HIV-1 infection of P4-treated cells was calculated based on untreated control representing 100% infection. Data are representative of the mean plus or minus SEM where $n = 3$ infection data points; $^*P < .05$. This figure is representative of 3 independent experiments

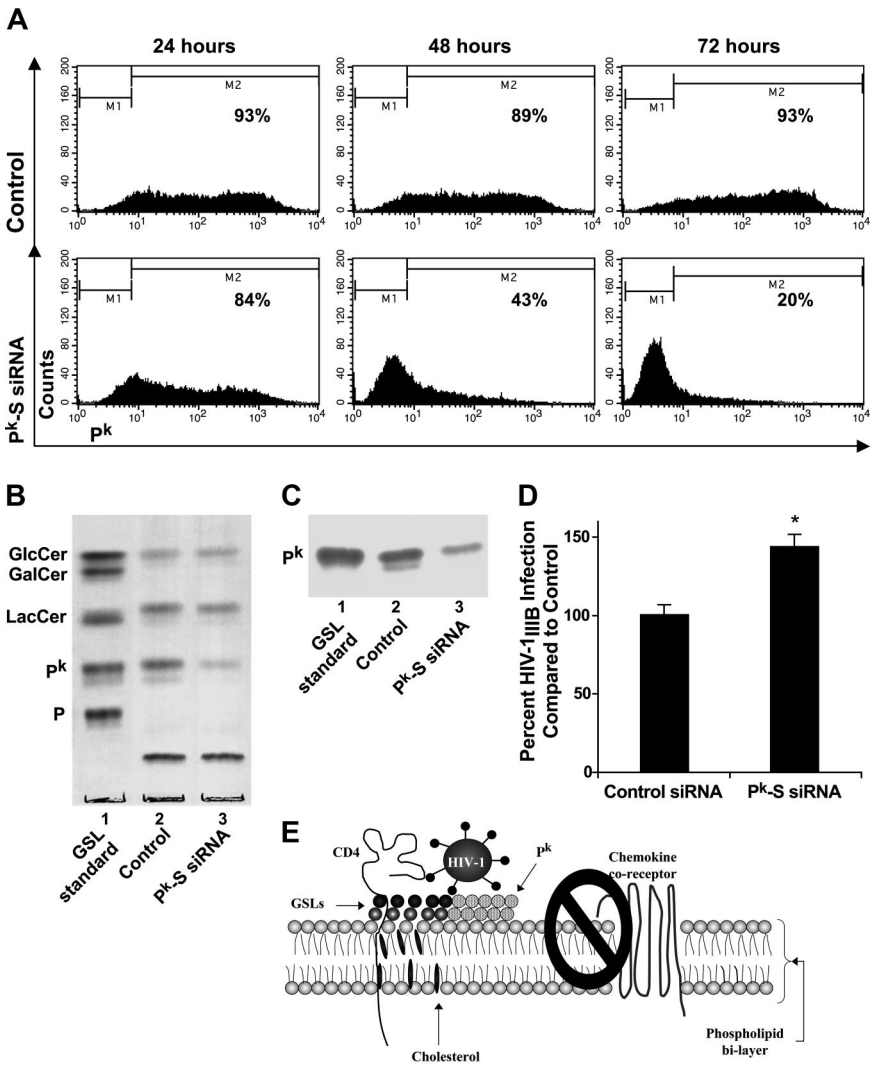

Figure 7. Specific depletion of Pᵏ correlates with increased HIV-1 infection. CD4⁺ HeLa cells (clone 6C) were transfected daily with either control siRNA or Pᵏ synthase (Pᵏ-S) siRNA, and cultured for 72 hours to deplete Pᵏ-S, and subsequently Pᵏ. FACS analysis was performed and scatter plots of CD4⁺ HeLa cells labeled with VT1B-Alexa$_{458}$ were analyzed, where background was compensated to unstained controls. (A) Histogram plots representing percentage of cell populations expressing Pᵏ. (B) TLC of total GSLs extracted from control and Pᵏ-S siRNA-transfected CD4⁺ HeLa cells. Lane 1: GSL standards. Lane 2: Control siRNA-transfected cells. Lane 3: Pᵏ-S siRNA-transfected cells. (C) VT1 overlay for Pᵏ detection was carried out on TLC of total GSLs Lane 1: GSL standards. Lane 2: Control siRNA-transfected cells. Lane 3: Pᵏ-S siRNA-transfected cells. (D) HIV-1$_{IIIB}$ (MOI, 0.3) infection of control (control siRNAs)- or Pᵏ-S siRNA-transfected CD4⁺ HeLa cells was measured by p24^{gag} production after 5 days of culture. Data are representative of the mean plus or minus SEM where n = 3 infection data points. $*P < .05$. This figure is representative of 3 independent experiments. (E) A schematic working model for Pᵏ-induced protection against HIV-1 infection. HIV first binds to CD4, which exposes the GSL and chemokine coreceptor binding site within the V3 loop of HIV gp120. When Pᵏ is highly expressed, it can successfully compete with chemokine coreceptor for the exposed sites within the V3 loop; thus, Pᵏ interferes with the process of membrane fusion.

Our studies indicate that susceptibility to HIV-1 infection in p PBMCs might be influenced both by the lack of Pᵏ antigen and by increased receptor and coreceptor expression; however, this is not the case with the P_1^k phenotype. P_1^k PBMCs demonstrated reduced susceptibility to R5 and X4 HIV-1 infection despite having increased expression of HIV-1 receptors. Thus, both rare p and P_1^k PBMCs showed increased patterns of HIV receptor and coreceptor expression, but this resulted in higher susceptibility to HIV infection only in the p PBMCs. Thus, Pᵏ expression was a better indicator of susceptibility to HIV-1 infection than CD4 or chemokine coreceptor expression.

Although the presence (or absence) of Pᵏ is important in blood group classification and transfusion medicine, Pᵏ is not restricted to erythrocytes. Pᵏ is expressed on monocyte populations, which encompass R5 HIV-1-susceptible target cells.[40,41] T-lymphoblasts mostly represent X4 HIV-1-susceptible target cell populations and have been reported to express little or no Pᵏ[40]; thus, T cells are similar to the p phenotype in their lack of Pᵏ expression, which may promote susceptibility to HIV-1 infection. Furthermore, variations in Pᵏ expression occur in the general population,[42] which could explain differences in susceptibility to HIV-1 infection seen in vitro and in vivo.

Differences in Pᵏ expression could influence lipid raft composition of target cell membranes and affect CD4 and/or coreceptor localization. Lipid rafts are central to HIV infection,[43] and CD4 and CCR5 are known to be associated with lipid rafts, whereas CXCR4 is not.[44] However, even CD4-HIVgp120-CXCR4 associations have been demonstrated within rafts and are required for membrane fusion.[45] If Pᵏ levels were able to influence appropriate localization of CD4 and/or coreceptors in lipid rafts, because of changes in the membrane milieu, this could affect target cell susceptibility to HIV-1.

Importantly, heightened susceptibility of cells without Pᵏ, and reduced susceptibility of cells that express increased Pᵏ, to both X4 and R5 HIV-1 infection would argue against current models, suggesting that Pᵏ is important in post-CD4-binding.[22] Increased GM3 has been proposed to promote membrane fusion in p-CD4⁺ T cells.[39] However, cell-surface expression and total GM3 do not correlate with enhanced PHA- or PHA/IL-2-activated PBMC HIV-1 infection in our study, although purified target cells remain to be assessed. It is clear, however, that Pᵏ is not an absolute requirement for membrane fusion and infection. HIV-gp120 binds Pᵏ via the V3 loop.[17,18,22] This loop also mediates chemokine receptor binding.[46,47] Thus, Pᵏ (or a soluble mimic[27]) binding to gp120 may interfere with post-CD4 recognition of chemokine coreceptor binding to prevent fusion and infection. Indeed, the binding motif, XXXGPGRAFXXX,[48] within the V3 loop for Pᵏ binding overlaps with the consensus binding motif, S/GXXXG-PGXXXXXXXE/D,[46] for chemokine coreceptors. It has also been shown that CD4 enhances gp120-Pᵏ interaction,[49] probably by a similar mechanism that allows for the interaction of chemokine

coreceptor with gp120 after CD4 binding.[50] Perhaps, under conditions of chemokine receptor deficiency (or the absence of CD4), P^k may thus (less efficiently) mediate viral internalization. However, when receptor levels are normal, and P^k is expressed at higher levels, P^k has the potential to interfere with the appropriate interactions between gp120 and chemokine coreceptors, thus inhibiting viral internalization (see Figure 7E for a working model).

The lack of P in P_1^k cells could suggest that P can facilitate, rather than P^k inhibit, infection. However, the high susceptibility of the p phenotype, which lack both P and P^k, makes this unlikely. In addition, gp120 binds P^k but not P.[15] Furthermore, the introduction of P^k by liposome transfer into a cell line deficient in P^k expression (providing a close representation to the p phenotype), confirmed the decrease in susceptibility to HIV-1 on increased P^k levels. The fact that introduction of P into this cell line does not affect HIV infection would argue against any ability to facilitate infection. Only the levels of P^k closely correlate to HIV susceptibility. This is further supported by use of a cell line, HeLa, which does not express P (Figure 7B), whereby after the introduction of the P^k synthase gene (α4Gal transferase), which increased the cell-surface expression levels of P^k was able to reduce HIV-1 infection. In addition, specific gene silencing using siRNAs to the P^k synthase gene resulted in increased HIV-1 infection.

In our previous study of Fabry patient samples,[26] which present intracellular P^k accumulation because of the lack of α-galactosidase A activity, we demonstrated a reduced susceptibility to HIV-1 infection. However, because we could only detect low levels of cell-surface expressed P^k, the mechanism of reduced HIV infection was unclear. This could have involved aspects of the abnormal pathology as a result of Fabry disease and/or abnormal trafficking of necessary coreceptors for HIV-1 infection.[26] Indeed, Fabry PBMCs only demonstrated a reduction in R5 HIV-1 infection, and CCR5 coreceptor was greatly decreased on the cell-surface of these patient samples. In contrast, in the current study, we show that HIV-1 infection directly correlates to increased or decreased cell-surface expression of P^k, and this is largely independent of CXCR4 or CCR5 coreceptor expression. When P^k is highly expressed on the cell surface, as is the case in P_1^k persons' PBMCs, infection with HIV-1 $\times$ 4 and R5 viruses is largely reduced. However, when there is no P^k cell-surface expression, such as in p persons' PBMCs, HIV-1 infection is potentially several logs greater than in cells having normal P^k cell-surface expression.

Although natural resistance factors to HIV infection have been actively sought, there have been no reports as yet of a cell-surface receptor that can provide a natural barrier to HIV infection.[1-4] The Δ32 polymorphism in the CCR5 chemokine cell-surface receptor that provides natural resistance to HIV infection is the result of a mutation that prevents the transport of this receptor to the cell surface. Thus, persons with this polymorphism do not express the receptor for R5 viruses on their cell surface.[2] We now provide the first evidence of a possible role for a naturally expressed cell-surface factor, the P^k GSL, as potentially providing some protection to both R5 and X4 strains of HIV-1. Although studies examining the incidence of the p and P_1^k phenotype in cohorts of HIV-infected, HIV-exposed but uninfected, HIV progressers and nonprogressers would be desirable, the frequency of these extremely rare phenotypes, estimated for p to be 5.8 per million, and with P_1^k much less frequent ($\sim$ 1 per million),[5,6] precludes these studies. Significantly, genetic studies identified chromosome 22q12-13 to be associated with HIV resistance,[51] and this region contains the P^k synthase gene[13] and HIV transgenic mice showed increased P^k synthesis.[52] To determine whether P^k cell-surface expression may indeed represent a natural resistance factor for HIV infection, population studies are required using normal cohorts with common P_1/P_2 phenotypes known to have differential P^k expression[42] to assess HIV-1 susceptibility in vitro. Furthermore, analyses of HIV-1-infected and HIV-1-resistant cohorts, using genetic and serologic/flow cytometric techniques are necessary. Nonetheless, based on our findings, P^k alone provides some protection to infection with HIV-1 and studies of modulation of P^k expression, by pharmacologic[29] or other intervention, may prove to be important for future HIV/AIDS treatment modalities.

Acknowledgments

The authors thank those donors whose PBMCs were used in this study, Mathieu Drouin for preparation of the P^k synthase–containing adenovector, and Dr Xiaolong Fan from Lund University for providing the Ad5/F35 adenovirus backbone.

This work was supported by the Canadian Blood Services through a graduate fellowship award (N.L.), the Canadian Institutes for Health Research via a Doctoral Research Award (N.L.) and operating grants, Canadian Institutes for Health Research (C.A.L., D.R.B.), the Ontario HIV Treatment Network (C.A.L., D.R.B.), the Canadian Association for HIV Research (C.A.L., D.R.B.), the Swedish Research Council (project no. K2005/2008-14251), the Medical Faculty of Lund University, governmental grants for clinical research to Lund University Hospital, and Region Skåne, Sweden (Å.H., M.L.O.).

Authorship

Contribution: N.L. performed experiments, analyzed data, and contributed to the writing of the manuscript; M.L.O. provided essential samples, analyzed data, and contributed to design of experiments and to the writing of the manuscript; Å.H. provided and characterized essential samples; S.R., D.S., and B.B. performed experiments; V.Y. and C.L. provided essential samples; X.-Z.M. and D.J. provided essential reagents and contributed to the writing of the manuscript; and C.A.L. and D.R.B. contributed to the design of experiments, analysis of the data, and the writing of the manuscript.

Conflict-of-interest disclosure: The authors declare no competing financial interests.

Correspondence: Donald R. Branch, Canadian Blood Services, Toronto General Research Institute, 67 College Street, Toronto, ON M5G 2M1 Canada; e-mail: don.branch@utoronto.ca.

References

1. Arenzana-Seisdedos F, Parmentier M. Genetics of resistance to HIV infection: role of coreceptors and coreceptor ligands. Semin Immunol. 2006; 18:387-403.
2. de Silva E, Stumpf MP. HIV and the CCR5-delta32 resistance allele. FEMS Microbiol Lett. 2004;241:1-12.
3. Paxton WA, Kang S. Chemokine receptor allelic polymorphisms: relationships to HIV resistance and disease progression. Semin Immunol. 1998; 10:187-194.
4. Moulds JM, Moulds JJ. Blood group associations with parasites, bacteria, and viruses. Transfus Med Rev. 2000;14:302-311.
5. Spitalnik PF, Spitalnik SL. The P blood group system: biochemical, serological, and clinical aspects. Transfus Med Rev. 1995;9:110-122.
6. Daniels G. Human Blood Groups. Malden, MA: Blackwell Science; 2002.
7. Lingwood CA. Role of verotoxin receptors in pathogenesis. Trends Microbiol. 1996;4:147-153.

8. Schwartz-Albiez R, Dorken B, Moller P, Brodin NT, Monner DA, Kniep B. Neutral glycosphingolipids of the globo-series characterize activation stages corresponding to germinal center B cells. Int Immunol. 1990;2:929-936.
9. Hellberg A, Poole J, Olsson ML. Molecular basis of the globoside-deficient P(k) blood group phenotype. Identification of four inactivating mutations in the UDP-N-acetylgalactosamine: globotriaosylceramide 3-beta-N-acetylgalactosaminyltransferase gene. J Biol Chem. 2002;277:29455-29459.
10. Hellberg A, Chester MA, Olsson ML. Two previously proposed P1/P2-differentiating and nine novel polymorphisms at the A4GALT (Pk) locus do not correlate with the presence of the P1 blood group antigen. BMC Genet. 2005;6:49.
11. Hellberg A, Ringressi A, Yahalom V, Safwenberg J, Reid ME, Olsson ML. Genetic heterogeneity at the glycosyltransferase loci underlying the GLOB blood group system and collection. Br J Haematol. 2004;125:528-536.
12. Furukawa K, Iwamura K, Uchikawa M, et al. Molecular basis for the p phenotype: identification of distinct and multiple mutations in the alpha 1,4-galactosyltransferase gene in Swedish and Japanese individuals. J Biol Chem. 2000;275:37752-37756.
13. Steffensen R, Carlier K, Wiels J, et al. Cloning and expression of the histo-blood group Pk UDP-galactose: Galpha1beta-4G1cbeta1-cer alpha1, 4-galactosyltransferase. Molecular genetic basis of the p phenotype. J Biol Chem. 2000;275:16723-16729.
14. Hellberg A, Steffensen R, Yahalom V, et al. Additional molecular bases of the clinically important p blood group phenotype. Transfusion. 2003;43:899-907.
15. Mylvaganam M, Lingwood CA. A convenient oxidation of natural glycosphingolipids to their "ceramide acids" for neoglycoconjugation: bovine serum albumin-glycosylceramide acid conjugates as investigative probes for HIV gp120 coat protein-glycosphingolipid interactions. J Biol Chem. 1999;274:20725-20732.
16. Fantini J, Hammache D, Delezay O, Pieroni G, Tamalet C, Yahi N. Sulfatide inhibits HIV-1 entry into CD4 super(-)/CXCR4 super(+) cells. Virology. 1998;246:211-220.
17. Hammache D, Pieroni G, Yahi N, et al. Specific interaction of HIV-1 and HIV-2 surface envelope glycoproteins with monolayers of galactosylceramide and ganglioside GM3. J Biol Chem. 1998;273:7967-7971.
18. Mahfoud R, Garmy N, Maresca M, Yahi N, Puigserver A, Fantini J. Identification of a common sphingolipid-binding domain in Alzheimer, prion, and HIV-1 proteins. J Biol Chem. 2002;277:11292-11296.
19. Dalgleish AG, Beverley PC, Clapham PR, Crawford DH, Greaves MF, Weiss RA. The CD4 (T4) antigen is an essential component of the receptor for the AIDS retrovirus. Nature. 1984;312:763-767.
20. Alkhatib G, Combadiere C, Broder CC, et al. CC CKR5: a RANTES, MIP-1alpha, MIP-1beta receptor as a fusion cofactor for macrophage-tropic HIV- 1. Science. 1996;272:1955-1958.
21. Feng Y, Broder CC, Kennedy PE, Berger EA. HIV-1 entry cofactor: functional cDNA cloning of a seven-transmembrane, G protein-coupled receptor. Science. 1996;272:872-877.
22. Nehete PN, Vela EM, Hossain MM, et al. A post-CD4-binding step involving interaction of the V3 region of viral gp120 with host cell surface glycosphingolipids is common to entry and infection by diverse HIV-1 strains. Antiviral Res. 2002;56:233-251.
23. Rawat SS, Viard M, Gallo SA, Rein A, Blumenthal R, Puri A. Modulation of entry of enveloped viruses by cholesterol and sphingolipids [Review]. Mol Membr Biol. 2003;20:243-254.
24. Puri A, Hug P, Jernigan K, Rose P, Blumenthal R. Role of glycosphingolipids in HIV-1 entry: requirement of globotriosylceramide (Gb3) in CD4/CXCR4-dependent fusion. Biosci Rep. 1999;19:317-325.
25. Brady RO, Gal AE, Bradley RM, Martensson E, Warshaw AL, Laster L. Enzymatic defect in Fabry's disease: ceramidetrihexosidase deficiency. N Engl J Med. 1967;276:1163-1167.
26. Lund N, Branch DR, Sakac D, et al. Lack of susceptibility of cells from patients with Fabry disease to productive infection with R5 human immunodeficiency virus. AIDS. 2005;19:1543-1546.
27. Lund N, Branch DR, Mylvaganam M, et al. A novel soluble mimic of the glycolipid, globotriaosyl ceramide inhibits HIV infection. AIDS. 2006;20:333-343.
28. Fantini J, Tamalet C, Hammache D, Tourres C, Duclos N, Yahi N. HIV-1-induced perturbations of glycosphingolipid metabolism are cell-specific and can be detected at early stages of HIV-1 infection. J Acquir Immune Defic Syndr Hum Retrovirol. 1998;19:221-229.
29. Ramkumar S, Sakac D, Binnington B, Branch DR, Lingwood CA. Induction of HIV-1 resistance: cell susceptibility to infection is an inverse function of globotriaosyl ceramide levels. Glycobiology. 2009;19:76-82.
30. Yousefi S, Ma XZ, Singla R, et al. HIV-1 infection is facilitated in T cells by decreasing p56lck protein tyrosine kinase activity. Clin Exp Immunol. 2003;133:78-90.
31. Branch DR, Valenta LJ, Yousefi S, et al. VPAC1 is a cellular neuroendocrine receptor expressed on T cells that actively facilitates productive HIV-1 infection. AIDS. 2002;16:309-319.
32. Bokaei PB, Ma XZ, Sakac D, Branch DR. HIV-1 integration is inhibited by stimulation of the VPAC2 neuroendocrine receptor. Virology. 2007;362:38-49.
33. Mattocks M, Bond M, Bagovitch M, et al. Treatment of the neutral glycosphingolipid lysosomal storage disease via inhibition of the ABC drug transporter, MDR1: cyclosporine A can lower serum and liver globotriaosyl ceramide levels in the Fabry mouse model. FEBS J. 2006;273:2064-2075.
34. Nutikka A, Binnington-Boyd B, Lingwood CA. Methods for the identification of host receptors for Shiga toxin. In: Philpot D, Ebel F, eds. Methods in Molecular Medicine, vol. 73, E. Coli Shiga Toxin Methods and Protocols. Totowa, NY: Humana Press; 2003;197-208.
35. Cayer MP, Drouin M, Sea SP, et al. Comparison of promoter activities for efficient expression into human B cells and haematopoietic progenitors with adenovirus Ad5/F35. J Immunol Methods. 2007;322:118-127.
36. Nilsson M, Ljungberg J, Richter J, et al. Development of an adenoviral vector system with adenovirus serotype 35 tropism: efficient transient gene transfer into primary malignant hematopoietic cells. J Gene Med. 2004;6:631-641.
37. GenBank, Kojima et al. http://www.ncbi.nlm.nih.gov/entrez/viewer.fcgi?db=nuccore&id=7959010. Accessed June 12, 2002.
38. Lee L, Abe A, Shayman JA. Improved inhibitors of glucosylceramide synthase. J Biol Chem. 1999;274:14662-14669.
39. Puri A, Rawat SS, Lin HM, et al. An inhibitor of glycosphingolipid metabolism blocks HIV-1 infection of primary T cells. AIDS. 2004;18:849-858.
40. Kiguchi K, Henning-Chubb CB, Huberman E. Glycosphingolipid patterns of peripheral blood lymphocytes, monocytes, and granulocytes are cell specific. J Biochem. 1990;107:8-14.
41. Kniep B, Monner DA, Schwulera U, Muhlradt PF. Glycosphingolipids of the globo-series are associated with the monocytic lineage of human myeloid cells. Eur J Biochem. 1985;149:187-191.
42. Fletcher KS, Bremer EG, Schwarting GA. P blood group regulation of glycosphingolipid levels in human erythrocytes. J Biol Chem. 1979;254:11196-11198.
43. Liao Z, Cimakasky LM, Hampton R, Nguyen DH, Hildreth JE. Lipid rafts and HIV pathogenesis: host membrane cholesterol is required for infection by HIV type 1. AIDS Res Hum Retroviruses. 2001;17:1009-1019.
44. Kozak SL, Heard JM, Kabat D. Segregation of CD4 and CXCR4 into distinct lipid microdomains in T lymphocytes suggests a mechanism for membrane destabilization by human immunodeficiency virus. J Virol. 2002;76:1802-1815.
45. Nguyen DH, Giri B, Collins G, Taub DD. Dynamic reorganization of chemokine receptors, cholesterol, lipid rafts, and adhesion molecules to sites of CD4 engagement. Exp Cell Res. 2005;304:559-569.
46. Xiao L, Owen SM, Goldman I, et al. CCR5 coreceptor usage of non-syncytium-inducing primary HIV-1 is independent of phylogenetically distinct global HIV-1 isolates: delineation of consensus motif in the V3 domain that predicts CCR-5 usage. Virology. 1998;240:83-92.
47. Sakaida H, Hori T, Yonezawa A, et al. T-tropic human immunodeficiency virus type 1 (HIV-1)-derived V3 loop peptides directly bind to CXCR-4 and inhibit T-tropic HIV-1 infection. J Virol. 1998;72:9763-9770.
48. Delezay O, Hammache D, Fantini J, Yahi N. SPC3, a V3 loop-derived synthetic peptide inhibitor of HIV-1 infection, binds to cell surface glycosphingolipids. Biochemistry. 1996;35:15663-15671.
49. Fantini J, Hammache D, Piéroni G, Yahi N. Role of glycosphingolipid microdomains in CD4-dependent HIV-1 fusion. Glycoconj J. 2000;17:199-204.
50. Kwong PD, Wyatt R, Robinson J, Sweet RW, Sodroski J, Hendrickson WA. Structure of an HIV gp120 envelope glycoprotein in complex with the CD4 receptor and a neutralizing human antibody. Nature. 1998;393:648-659.
51. Kanari Y, Clerici M, Abe H, et al. Genotypes at chromosome 22q12-13 are associated with HIV-1-exposed but uninfected status in Italians. AIDS. 2005;19:1015-1024.
52. Liu XH, Lingwood CA, Ray PE. Recruitment of renal tublular epithelial cells expressing verotoxin-1 (Stx1) receptors in HIV-1 transgenic mice with renal disease. Kidney Int. 1999;55:554-561.